Proceedings of The Canadian Society for Mechanical Engineering International Congress 2018
CSME International Congress 2018
May 27-30, 2018, Toronto, ON, Canada

Evaluation of Anti-Icing Polymer Coatings

Nick Tepylo and Xiao Huang
Carleton University, Dept. of Mechanical and Aerospace Engineering

Marc Budinger
University of Toulouse, Institut Clément Ader (ICA), INSA
Pierrick Rouset and Valérie Pommier-Budinger
University of Toulouse, ISAE SUPAERO

Abstract— Ice accumulation on aircraft, wind turbines and power lines can have detrimental effects, including efficiency reduction, mechanical failures and the creation of safety hazards. The aim of this study is to investigate the ice adhesion and wear resistance of three hydrophobic and icephobic coatings applied onto an aluminum substrate. Ethylene-tetrafluoroethylene (ETFE) coating was deposited using a plasma spray method while advanced liquid glass (ALG) and silicone R-2180 were both applied using dipping followed by furnace curing. Water was applied and frozen between both bare and coated surfaces using a custom built jig at -20 °C for 24 hours. The ice adhesion strength was measured using a lap shear test done inside an insulated chamber. The results showed low ice adhesion strengths for both ALG and silicone R-2180 coatings when compared to the bare surface. It was also found the silicone R-2180 coating had a higher wear rate than both the ETFE and ALG coatings. By combining icephobic coatings with an ultrasonic de-icing system, the power required by the system can be reduced, creating a low-powered active approach to the de-icing problem.

Keywords *- anti-icing, coatings, ultrasonic de-icing system, ice adhesion*

I. INTRODUCTION

Ice accumulation and wet-snow adhesion to solid outdoor surfaces can cause severe accidents and large economic losses. Such problems are present in many fields, from aeronautics [1] to off-shore oil platforms [2] and from power lines [3] to wind turbines [4]. On aircraft, ice accumulation can result in decreased lift, increased drag, decreased thrust, reduced stall angle, altered stall characteristics and even engine failure due to ice shedding. Aircraft icing can occur both during flight and on the ground. It has led to many reported aircraft accidents including Air Florida Boeing 737 (1982) and the American Eagle ATR 72 (1997). To ensure aircraft safety, regulatory bodies such as the FAA, JAA and EASA have established regulations for anti-icing and de-icing measures.

Present-day anti-icing and de-icing strategies can be chemical, thermal, electrical, and mechanical. Chemical methods belong to the passive techniques and can be used for anti-icing and de-icing. They can be categorized into freezing point depressants or icephobic/hydrophobic coatings. Freezing point depressants lower the freezing point of water which prevents the freezing of supercooled water droplets or creating a thin film of water between the aircraft surface/ice interface to assist ice-shedding. Viscous icephobic/hydrophobic coatings adhere to the surface, creating a thin film promoting ice-shedding. Chemicals can only be employed as an effective anti-icing strategy when being applied just prior to takeoff and reapplied for whenever the possibility of ice accretion exists on the ground. Corrosion becomes an issue with sodium chloride based inorganic freezing point depressants while organic anti-icing and de-icing chemicals (such as propylene glycol) have the potential to provide better snow and ice control performance and are less corrosive. However, organic materials are generally more costly and may be subject to dilution and pose environmental concerns.

The active methods depend on an external action being applied such as thermal, electro-thermal, electro-mechanical, or electromagnetic, and, as for passive methods, rely on the physical properties of the solid surface [5]. Thermal methods are based on the extraction of hot air from the engine, but this bleed reduces the efficiency of the engine. An electro-thermal de-icing system was adopted by Boeing in the B787 but this solution is energy-intensive. Mechanical devices such as pneumatic boots which break the accumulated ice by inflating can be implemented but these boots have a significant impact on the aerodynamics of the aircraft and a low durability. Finally, electromagnetic technologies based on the deformation of a winding are penalized by the weight of the power supply.

All of these existing methods entail disadvantages (cost, environmental concerns, large amount of power required). As such, the aviation industry is searching for a more efficient and cost-effective means for de-icing and anti-icing [6].

The authors advocate the use of hydrophobic and icephobic coatings in conjunction with electro-mechanical ice protection systems. The active ice protection systems generate shear stresses at the interface between the ice and the structure to break the accumulated ice and this shear stress required for ice shedding is reduced by the coating, which reduces the power

required by the actuators, and also the size and weight of the overall system. Based on the published literature, two main coating types can lessen the effect of ice accumulation. The first type contributes to the so called icephobic materials [7-10]. Such material reduces the shear forces required to break the accumulated layer of ice on the solid surface. The second type focuses on hydrophobic features. Surfaces coated with hydrophobic materials have a high tendency in repelling water due to the high contact angle between the water droplet and the solid surface. Hence this method eliminates the accumulation of water before water freezes and ice formation occurs. In the present study, two hydrophobic coatings (Ethylene-tetrafluoroethylene (ETFE), advanced liquid glass (ALG)) and one icephobic coating (silicone R-2180) were applied onto the aluminum (Al) 2024 substrate and tested for ice adhesion strength and wear resistance. These coatings were selected to experiment with different coating application methods and surface properties.

II. Materials and Experimental Procedures

A. *Sample Preparation*

The substrate material used in this study was Al 2024-T3 cut to a size of 75 mm by 25 mm for ice adhesion testing and a 25 mm by 25 mm section for the wear test. Four different surface conditions were investigated. A sandblasted (SB) coupon with no coating, a SB coupon with ethylene-tetrafluoroethylene (ETFE from Dupont) plasma sprayed coating, a SB coupon with an Advanced Liquid Glass (ALG, from Liquid Glass Shield) coating, and a SB coupon with silicone R-2180 (Nusil Technology). ETFE is similar to PTFE as they are both hydrophobic and composed of a carbon chain with fluorine reaction groups while ALG is a hydrophobic low friction coating with added silica particles. For ice adhesion tests, coating was applied only to 25 mm by 25 mm section of the coupon.

During the plasma spraying of ETFE, a mixture of 20% nitrogen gas and 80% argon was used as the carrier gas. The aluminum coupons were preheated for two minutes by the plasma stream before spraying. Other spraying parameters for ETFE coupons consisted of 190 A arc current, 220 slm argon gas flow rate and 100 mm offset distance between the nozzle and the coupons. After coating, all ETFE coupons were baked at 274°C for 20 minutes as recommended by the supplier [11].

The other two coatings, ALG and silicone R-2180, were applied using dipping application. Samples were dipped into a beaker containing ALG for 5 seconds and were cured in an air furnace at 250 °C for 1 hour. For the silicone R-2180 coating, the samples were dip coated and allowed to cure at room temperature for 30 minutes, then were placed in a furnace at 75 °C for 45 minutes and subsequently the temperature was increased to 150 °C and cured for another 135 minutes.

B. *Ice Adhesion Test*

A freezing jig was manufactured to hold the coupons in place during the freezing process. The jig was designed such that the gap clearance between the top and bottom coupons remains constant at 1 mm. The jig shown in Figure 1 uses slots to keep the coupons aligned and can hold six test specimens at once (a total of 12 coupons). A layer of parafilm was placed on top of the jig to prevent the coupons from sticking to the surface of the jig during the freezing process. Using a 1 mL syringe, 0.6 mL of deionized water was then injected into the hole in the lap shear joint (25 mm overlap) and the jig was placed in a freezer for 24 hours. This was done to ensure a complete transition of water to ice between the two coated surfaces. After 24 hours, each specimen was removed and inspected to ensure complete formation of ice between the coated surfaces.

Figure 1: (a) As fabricated jig used to align lap shear samples during freezing and (b) jig with sample loaded.

The ice adhesion test was carried out using a Material Testing System (MTS) to measure the force required to break the lap joint. From the measured force, the shear stress at which ice is detached from the surface can be determined. The frozen specimen was placed inside an insulated chamber and gripped by the MTS. The chamber kept the specimens at a temperature of approximately -20 °C for the duration of the test. The test setup can be found in Figure 2(a) while the inside of the chamber is shown in Figure 2(b). An axial displacement rate of 1 mm/min was used to pull the joint apart. The maximum load was then recorded for each sample.

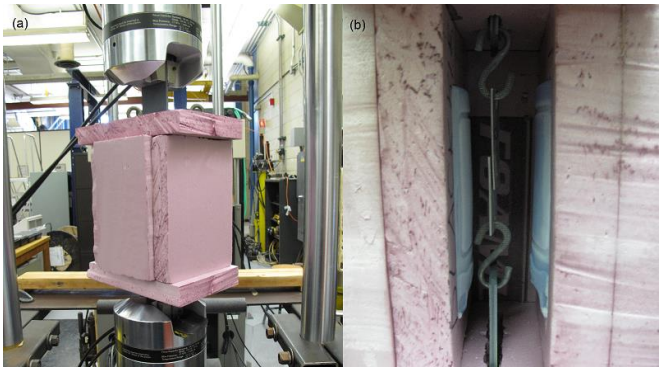

Figure 2: (a) Insulated chamber shown in the MTS and (b) cross-section of the insulated chamber with a loaded sample.

In order to compare the results obtained, the adhesion reduction factor (ARF) was used and is calculated using the following equation:

$$ARF = (\tau_{aluminum}/\tau_{coating}) \quad (1)$$

where $\tau_{aluminum}$ is the shear stress of the bare aluminum sample and $\tau_{coating}$ is the shear stress in the coated sample being investigated. A high ARF value corresponds to a coating that has a low ice adhesion strength when compared to aluminum [12].

C. Maintaining the Integrity of the Specifications

A pin-on-disk wear test was carried out to compare the coating's resistance to wear. It was performed under the dry sliding condition, according to ASTM 99-05 using a wear tester with model No: NEO-TRIBO MPW110 provided by NEOPLUS. This apparatus uses a rotating pin pressed under a normal force of 24.5 N against a static coating sample. The pin used was a Teflon ball with a radius of 2.5 mm. During the test, the specimen was placed horizontally with its center at a distance of 5 mm away from the vertical axis of the pin shaft. The pin (ball) was spinning at a constant speed of 50 RPM. As the result of friction/wear, a 10 mm diameter circular wear track was generated on the specimen surface. Wear loss of the coating material was measured based on the track depth. A new Teflon ball was used for each test to eliminate cross contamination between samples.

III. RESULTS

A. Ice Adhesion Strength Results

The lap shear test results are presented in Table 1. The bare, sandblasted aluminum samples required on average 447 kPa to shear the ice between the two coupons. This indicates that the bare sand blasted coupons exhibited a stronger adhesion to ice than the other coatings tested in this study.

Table 1: Adhesion strength for tested coatings

Coating	Adhesion Strength (kPa)	ARF
Sandblasted Al	447 ± 71	-
ALG	151 ± 69	2.96
ETFE	357 ± 72	1.25
R-2180	187 ± 26	2.39

A total of six samples were shear tested for each type of the coatings. A large variation was observed in the results obtained from this study. However, these variations in adhesion strength for each coating group are similar and also comparable that from previous tests conducted by other researchers. The ice adhesion strength of aluminum has been measured as low as 242 kPa [13] and sandblasted aluminum has been measured at 610 kPa [14]. In a similar experiment carried out using a lap joint shear test conducted in an MTS, the ice adhesion strength of the bare aluminum 2024 sample was 399.7 kPa [15] which closely resembles the 447 kPa obtained in this study. Although the results of this study do not closely match previous work [2], the ARF instead acts as a comparison tool for the tested coatings. ALG had the highest tested ARF of 2.96, followed by R-2180 (2.39) and ETFE (1.25).

There are several variables that could not be controlled during the testing and lead to deviations in the results. Any deviation in terms of actual ice temperature would have an impact on the required shear force. Another variable is the clamping pressure used during freezing. While the position of the clamps was constant for freezing each sample, the pressure exerted on each sample could be different due to the effects of the surface tension exerted by the water. Since each surface is different in the surface tension can vary significantly and cause a difference in the adhesion of ice to the sample.

B. Wear Resistance Results

A pin on disc wear test was used to evaluate the wear resistance of the three coatings using the procedure described previously. After the wear testing was conducted, SEM images were obtained to assess the damage to the coatings. The amount of wear was dependent on the type of coating and the duration of the test. Each coating was tested for durations of 1, 2, 4 and 8 minutes. A graph showing the wear loss, in terms of wear depth tracked by the location of the pin, of the three coatings plotted against the number of cycles can be found in Figure 3. ETFE wears at a rate of approximately twice the rate of the ALG samples while the silicone R-2180 samples wear out approximately six times more than the ALG samples.

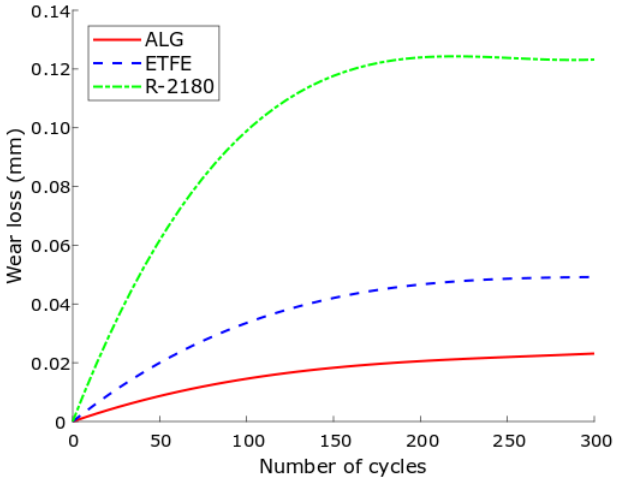

Figure 3: Wear loss for the ALG (red), ETFE (blue) and silicone R-2180 (green) samples.

As the test duration increased, the wear rate of each coating decreased. This can be expected as the longer the test lasts, the Teflon ball comes into contact with more coating surface area and a larger force is required to displace the coating. ALG coating, being a primarily SiO_2 based, was the most resistive to wear. The silicone R-2180 is an elastomer-based coating

and is fairly soft so the ball could easily displace the coating along the wear track. There was also a net mass increase in each sample due to the deposition of Teflon flakes from the pin onto the sample. As the surface of the pin was in contact with the coating, flakes wore off from the tip and were left along the wear track. Figure 4 shows the flakes that were deposited into R-2180 coating that was tested for 4 minutes.

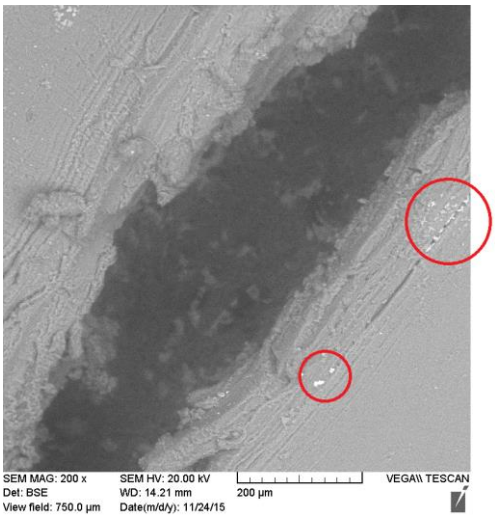

Figure 4: Teflon flakes were deposited into the wear track.

C. Feasibility for anti-icing applications

A composite plot was created in order to aid the selection process of anti-icing coatings for industrial applications. This plot is shown in Figure 5. As can be seen on the plot, ALG has the combination of the highest ARF and the lowest wear loss making it the most suitable coating for anti-icing applications. Coatings in the contained region possess a high ARF and low wear rate relative to other tested coatings. Coatings outside of this region are not suitable for aircraft as they possess either an ARF that is low when compared to other coatings or can wear quickly, exposing the surface of the aircraft.

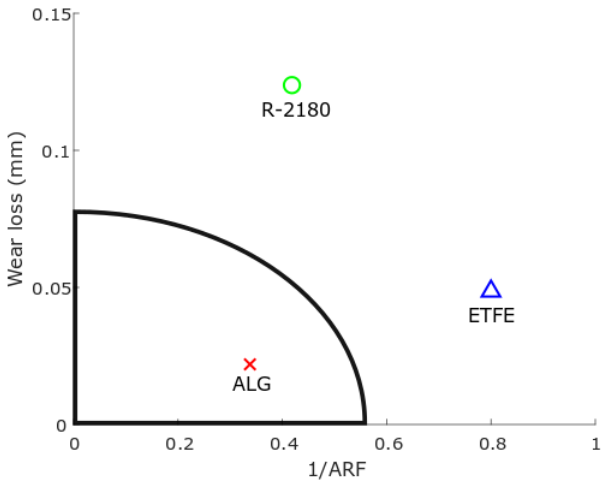

Figure 5: Composite plot of ARF and wear loss for the tested coatings.

D. Potential for combined anti-icing coating and ultrasonic de-icing systems

The potential exists to combine icephobic coatings with pre-existing de-icing systems to reduce the ice adhesion strength on the surface, which results in lower power consumption. Budinger *et al.* experimented with ultrasonic de-icing systems and developed a model to calculate the stress in the piezoceramic and the required voltage and current needed to delaminate a sheet of ice [16]. It was shown that the voltage and current required for delamination are linearly related to the ice adhesion strength [6]. Thus, the power required to delaminate a sheet of ice is proportional to the square of the ice adhesion strength, which means that an ARF of two would cause the power to decrease by a factor of four, reducing the size of actuator needed for the system.

Listed in Table 2 are the ARF of the tested coatings and the theoretical reduction in power due to the coating being used in conjunction with the ultrasonic de-icing system. Further decreases in the power can be achieved using icephobic coatings with a higher ARF.

Table 2: Power reduction factor when the coating is combined with an ultrasonic de-icing system

Coating	ARF	Power Reduction Factor
ALG	2.96	8.76
R-2180	2.39	5.71
ETFE	1.25	1.56

The proposed system is shown in Figure 6. Several piezoelectric actuators are positioned on the inside of the leading edge of the aircraft while an icephobic coating is applied on the exterior. The size and quantity of the actuators is dependent on the ARF of the selected coating. The system is similar to the Low Frequency De-Icing system (LFDI) proposed by Endres et al. [17] with the surface having a lower ice adhesion strength due to the icephobic coating.

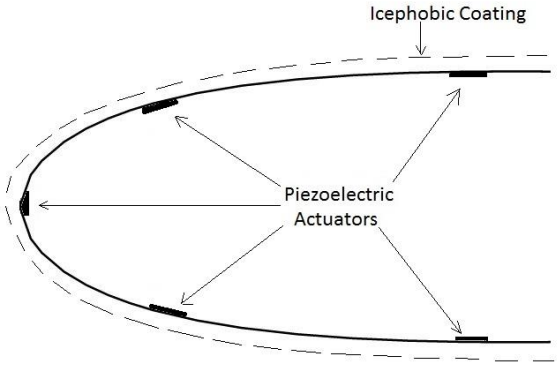

Figure 6: Proposed ice protection using both icephobic coating and piezoelectric actuators.

IV. CONCLUSIONS

Ice accretion on aircraft can have catastrophic consequences and the aviation industry is looking for both passive and active approaches to prevent and eliminate ice accretion. Ice adhesion was studied on four types of surfaces with different characteristics in order to analyze their icephobic properties. Ice adhesion strength measurements were obtained using an MTS and a constant axial displacement rate. The ALG coating decreased the ice adhesion by a factor of 2.96 and the silicone R-2180 reduced the ice adhesion strength by a factor of 2.39 when compared to an uncoated aluminum substrate. In addition to analyzing the icephobic characteristics of coatings, the durability in terms of wear was also assessed to validate its continuous effectiveness against ice. The R-2180 coating wore off easily compared to the ETFE and ALG coatings. As such, ALG coating was found to be a more suitable coating for the anti-icing application as it would not need to be consistently reapplied while having the highest ARF.

By selecting a coating with a high ARF and a low wear rate, the coating can be coupled with ultrasonic de-icing systems and provide an effective solution to de-icing. The relationship between the ARF and reduction in power is exponential, which makes the ARF a critical factor when selecting a coating.

ACKNOWLEDGMENT

The authors would like to acknowledge Ayman Ibrahim and Fred Barrett for developing the plasma spray process used to coat ETFE samples.

REFERENCES

[1] A. Heinrich, R. Ross, G. Zumwalt, J. Provorse, V. Padmanabhan, J. Thompson, and J. Riley, Aircraft Icing Handbook - Volume 3 of 3. Gates Learjet Corporation, 1991.

[2] C. C. Ryerson, “Assessment of superstructure ice protection as applied to offshore
oil operations safety," Tech. Rep. CRREL TR-09-4, U.S. Army Cold Regions Research and Engineering Laboratory, Hanover, New Hampshire 03755, April 2009.

[3] J. Laforte, M. Allaire, and J. Laflamme, “State-of-the-art on power line de-icing," *Atmospheric Research*, vol. 46, pp. 143-158, 1998.

[4] R. Karmouch, S. Coudé, G. Abel, and G. Ross, “Icephobic PTFE coatings for wind turbines operating in cold climate conditions." INRS-Centre Énergie Matériaux Télécommunications, Varennes (Québec) J3X 1S2 Canada.

[5] N. Dalili, A. Edrisy, and R. Carriveau, “A review of surface engineering issues critical to wind turbine performance," *Renewable and Sustainable Energy Reviews*, vol. 13, pp. 428-438, 2009.

[6] M. Budinger, V. Pommier-Budinger, G. Napias, and A. Costa da Silva, “Ultrasonic ice protection systems: Analytical and numerical models for architecture tradeoff," *Journal of Aircraft*, vol. 68, pp. 91-98, 2016.

[7] KISS Polymers LLC. Product Summary. http://www.kisspolymers.com/index.htm. [Online; Accessed 12-June-2016]. 2008.

[8] N. D. Mulherin and R. Haehnel, “Progress in Evaluating Surface Coatings for Icing Control at Corps Hydraulic Structures,” Tech. Rep. Ice Engineering Information Exchange Bulletin, TN-03-4, U.S. Army Cold Regions Research and Engineering Laboratory, Hanover, New Hampshire 03755, 2003.

[9] R. Menini and M. Farzaneh, “Elaboration of Al2O3/PTFE icephobic coatings for protecting aluminum surfaces," *Surface and Coating Technology*, vol. 203, pp. 1941-1946, 2009.

[10] J. E. Mark, “Some interesting things about polysiloxanes," *Accounts of Chemical Research*, vol. 37, pp. 946-953, 2004.

[11] DuPont Teflon®. Non-stick and Industrial Coatings. http://www.intechservices.com/Teflon-Product-Overview. [Online; Accessed 12-June-2016]. 2015.

[12] M. Susoff, K. Siegmann, C. Pfaffenroth, and M. Hirayama, “Evaluation of ice-phobic coatings-screening of different coatings and influence of roughness," *Applied Surface Science*, vol. 282, pp. 870-879, 2013.

[13] F. Arianpour, M. Farzaneh, and R. Jafari, “Hydrophobic and ice-phobic properties of self-assembled monolayers (SAMs) coatings on AA6061," *Progress in Organic Coatings*, vol. 93, pp. 41-45, 2016.

[14] M. Zou, S. Beckford, R.Wei, C. Ellis, G. Hatton, and M. Miller, “Effects of surface roughness and energy on ice adhesion strength," *Applied Surface Science*, vol. 257, pp. 3786-3792, 2011.

[15] B. Dixon, A. Walsh, B. Gall, and M. Goodwin, “Novel phase change material icephobic coating for ice mitigation in marine environments," in Green Ships, Eco Shipping, Clean Seas, The 12th Annual General Assembly of IAMU, 2014.

[16] V. Pommier-Budinger, M. Budinger, N. Tepylo, and X. Huang, “Analysis of Piezoelectric Ice Protection Systems Combined with Ice-Phobic Coatings," in *8th AIAA Atmospheric and Space Environments Conference*, pp. 623-628, 2016.

[17] M. Endres, H. Sommerwerk, C. Mendig, M. Sinapius, and P. Horst, “Experimental Study of two Mechanical De-Icing Systems Applied on a Wing Section tested in an Icing Wind Tunnel,” German Aerospace Congress 2016, (Braunschweig, Germany), September 2016.